Impact of Self-Heating on the Statistical Variability in Bulk and SOI FinFETs

Liping Wang, Andrew R. Brown, *Member, IEEE*, Mihail Nedjalkov, Craig Alexander, Binjie Cheng, *Member, IEEE*, Campbell Millar, *Member, IEEE*, and Asen Asenov, *Fellow, IEEE*

***Abstract*— In this paper, for the first time, we study the impact of self-heating on the statistical variability of bulk and Silicon-on-insulator FinFETs designed to meet the requirements of the 14/16-nm technology node. The simulations are performed using the Gold Standard Simulations atomistic simulator GARAND using an enhanced electrothermal model that considers the impact of the fin geometry on the thermal conductivity. In the simulations, we have compared the statistical variability obtained from full-scale electrothermal simulations with the variability at uniform room temperature and at the maximum or average temperatures obtained in the electrothermal simulations. The combined effects of line edge roughness and metal gate granularity are considered. The distributions and the correlations between key figures of merit, including the threshold voltage, ON-current, subthreshold slope, and leakage current are presented and analyzed.**

***Index Terms*— CMOS, correlations, electrothermal simulations, FinFETs, statistical variability.**

I. Introduction

FinFETs enable technology scaling at the 22-nm CMOS technology generation and beyond because of their excellent electrostatic integrity and control of short channel effects [1]. This is complemented by lower statistical variability due to a tolerance of lower channel doping compared with bulk transistors. Self-heating has been highlighted as one of the areas of concern for FinFETs because of the 3-D geometry, the impact of the corresponding 3-D heat flow through the fin to the substrate and the impact of the fin geometry on the local thermal conductivity [2]–[8]. These perceived self-heating problems could be exacerbated in Silicon-on-insulator (SOI) FinFETs where the thermal conduction toward the substrate is impeded by the low thermal conductivity of the SOI layer beneath the fin [7]. Therefore, analyzing and modeling the self-heating in FinFETs and the influence on device performance have become one of the topics attracting a lot of recent interest [2]–[8].

At the same time, statistical variability introduced by the discreteness of charge and matter has become critically important in contemporary and future CMOS technologies [9]–[10]. In particular, the impact of random discrete dopants, fin line edge roughness (LER), gate line edge roughness (GER), and metal gate granularity (MGG) on the variability in bulk and SOI FinFETs have been studied in detail previously [11]. However, to the best of our knowledge, the impact of self-heating has not to be considered before in such simulation studies.

In this paper, we use the enhanced self-heating simulation capabilities, recently introduced in the Gold Standard Simulations (GSS) atomistic device simulator GARAND [8], [12], complemented by the unique capabilities for physical simulation of different sources of statistical variability [13], [14], to study, for the first time, the impact of self heating on FinFET variability. The test-bed transistors in this paper are bulk and SOI FinFETs designed to meet the specifications for the 14/16-nm CMOS technology generation [11].

This paper is organized as follows. In Section II, we briefly describe the bulk and the SOI FinFETs used as demonstrators in this paper. Section III presents the simulation technology including the enhanced electrothermal simulation method in more detail along with the physical statistical simulation capabilities. The results and analysis of statistical variability in the presence of self-heating effects are presented in Section IV. Finally, the conclusions are drawn in Section V.

II. Testbed Transistors

Two n-channel FinFETs, which are on SOI and bulk substrates, respectively, but have identical dimensions, are used as a test bed in our investigation. Their schematic structures are shown in Fig. 1. The nominal device parameters are listed in Table I. For the bulk FinFET, a 5×10^{18} cm^{-3} channel stop doping is introduced below the channel. A conservative channel length of $L_G = 25$ nm was assumed. A high-k gate dielectric is used to minimize gate leakage. Table II compares the key figures of merit of the two transistors, which are very similar in terms of performance.

III. Simulation Methodology

A. Electrothermal Simulations

Within the framework of the GSS statistical-variability-aware device simulator GARAND [12], we have developed

Manuscript received December 10, 2014; revised April 21, 2015; accepted May 13, 2015. Date of publication June 4, 2015; date of current version June 17, 2015. This work was supported by the European Union through the Seventh Framework Programme (FP7/2007-2013) within the SUPERTHEME Project under Grant 318458. The review of this paper was arranged by Editor Y. Momiyama.

L. Wang is with the School of Engineering, University of Glasgow, Glasgow G12 8LT, U.K. (e-mail: liping.wang@glasgow.ac.uk).

A. R. Brown, C. Alexander, B. Cheng, and C. Millar are with Gold Standard Simulations Ltd., Glasgow G12 8LT, U.K. (e-mail: a.brown@goldstandardsimulations.com; c.alexander@goldstandardsimulations.com; b.cheng@goldstandardsimulations.com; c.millar@goldstandardsimulations.com; asen.asenov@glasgow.ac.uk).

M. Nedjalkov is with the Institute for Microelectronics, Technische Universität Wien, Vienna 1040, Austria (e-mail: nedialkov@iue.tuwien.ac.at).

A. Asenov is with the School of Engineering, University of Glasgow, Glasgow G12 8LT, U.K. and also with Gold Standard Simulations Ltd., Glasgow G12 8LT, U.K. (e-mail: asen.asenov@glasgow.ac.uk).

Color versions of one or more of the figures in this paper are available online at http://ieeexplore.ieee.org.

Digital Object Identifier 10.1109/TED.2015.2436351

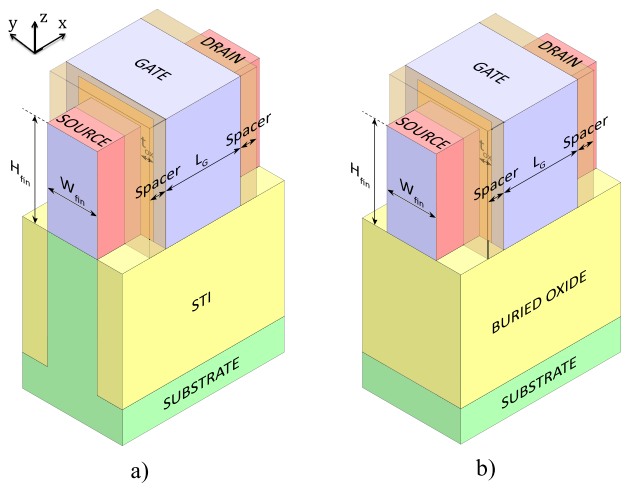

Fig. 1. Schematic of (a) bulk and (b) SOI FinFETs.

TABLE I
NOMINAL DEVICE PARAMETERS

Parameter	Value
L_G	25 nm
Fin Width, W_F	12 nm
Fin Height, H_F	30 nm
Spacer	6 nm
Extension	No extension doping
highly doped drain (HDD) profile	2nm/dec (σ=2.1nm)
highly doped drain (HDD) doping	1×10^{20} cm^{-3}
Equivalent Oxide Thickness (EOT)	0.8 nm
Channel stop doping	5×10^{18} cm^{-3}
Channel doping	1×10^{15} cm^{-3}
BOX / STI depth	30 nm
Supply Voltage	0.9 V

TABLE II
KEY FIGURES OF MERIT OF THE TWO TRANSISTORS

	Bulk FinFET	SOI FinFET
VTlin (Volts)	0.286	0.294
VTsat (Volts)	0.254	0.258
SS (mV/decade)	69.8	71.1
DIBL (mV)	31.6	36.8
IDlin (mA/μm)	0.342	0.360
IDsat (mA/μm)	1.177	1.244

a thermal simulation module to investigate the impact of self-heating on FinFET dc operation and on the corresponding statistical variability. This module is based on the solution of the coupled heat flow, poisson, and current continuity equations [8].

Usually, the electrical characteristics of the device are calculated in a restricted device simulation domain in order to maximize computational efficiency. However, heat is dissipated in a much larger domain, including the active region of the transistor, its neighbors, the substrate, the interconnect layers, the case, and eventually the heat sink. Therefore, realistic thermal boundary conditions rely on thermal resistances, employed to account for heat dissipation into interconnects, the wafer, the case, and so on. For given values

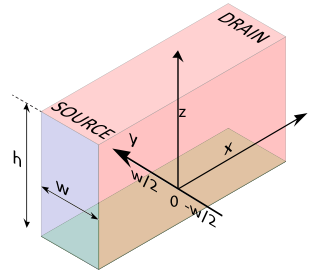

Fig. 2. Fin of height h and width w. The z-axis is along the direction of fin height with the bottom and top surfaces of the fin being at $z = 0$ and $z = h$, and the y-axis is along the direction of fin width with the surfaces of the fin being at $y = -w/2$ and $y = w/2$.

of thermal resistances, GARAND calculates the temperature differences using an iterative scheme according to the temperature gradient until convergence is achieved.

Since the fin thickness (width) is of the order of 10 nm, the thermal conductivity can be significantly reduced compared with bulk Si due to phonon-boundary scattering. We employ a new approximate formula for the calculation of the thermal conductivity in the fin region, which extends the previous 1-D formula [15] to 2-D [8]. Considering a fin of height h and width w as shown in Fig. 2, the thermal conductivity of the fin is given by

$$\kappa(y,z,T) = \kappa_0(T)\int_0^{\pi/2}\sin^3\theta\left\{1-\exp\left(-\frac{h}{2\lambda(T)\cos\theta}\right)\times\cosh\left(\frac{h-2z}{2\lambda(T)\cos\theta}\right)\right\}d\theta \times\int_0^{\pi/2}\sin^3\theta\left\{1-\exp\left(-\frac{w}{2\lambda(T)\cos\theta}\right)\cosh\left(\frac{-2y}{2\lambda(T)\cos\theta}\right)\right\}d\theta \quad (1)$$

where y and z are the coordinates, T is the lattice temperature, $\lambda(T)$ is phonon mean free path with temperature dependence, $\kappa_0(T)$ is the parameterized bulk thermal conductivity with temperature dependence, and θ is the integral variable.

Using this new calculation method, the thermal conductivity of the fin is predicted to be 1–2 orders of magnitude lower than the conventional value of the thermal conductivity for bulk Si. In our electrothermal simulation module, the thermal conductivity at each mesh point in the fin is refreshed according to its spatial position and temperature at each iteration cycle, which ensures the self-consistency of the simulation. By using this formula, the thermal conductivity and lattice temperature in a slice of the fin which is 5 nm below the top gate in the SOI FinFET example, resulting from the self-consistent simulations are shown in Fig. 3. The thermal conductivity in the middle of the fin is 0.027 W/(cm K). Currently, the parameters are adopted from [15], which can be recalibrated if novel experimental data for a nanoscale fin structure become available in the literature. The anisotropy of thermal conductivity is not included in this paper, but will be considered at a future stage.

In the electrothermal simulations of the bulk and SOI FinFETs, at the bottom of the simulation domain and at the top of the source and drain contacts external thermal resistances are employed and the temperature at these

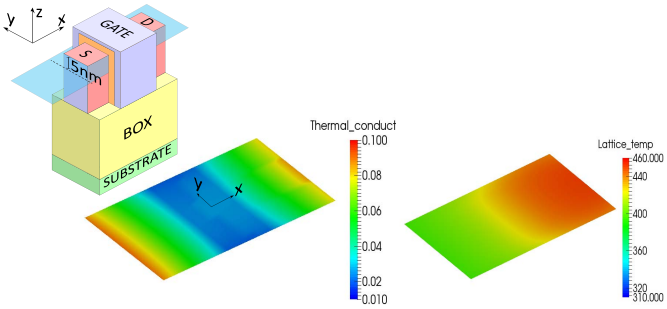

(a) (b)

Fig. 3. (a) Thermal conductivity and (b) lattice temperature in a slice of the fin which is 5 nm below the top gate in the SOI FinFET example, at $V_g = V_d = 0.9$ V, finally obtained from the self-consistent simulation. Inset: schematic showing the cut plane.

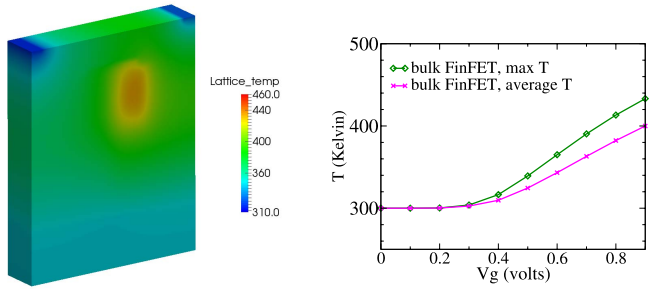

(a) (b)

Fig. 4. Simulation results for the bulk FinFET. (a) Lattice temperature profile in the middle at $V_g = V_d = 0.9$ V. (b) Maximum temperature and average temperature in the fin at high drain voltage.

boundaries is calculated according to the values of thermal resistances and heat flow. 2×10^6 K/W substrate thermal resistance and two 1×10^6 K/W contact thermal resistances have been used in this case based on rough estimation. The external thermal resistances are user-specified parameters for the electrothermal simulation module. The values used here are just for demonstration. A good estimation for external thermal resistances should consider the bulk resistance, interface resistances, effects of heat radiation, and spreading. The Masetti model [16] is used for doping-dependent low-field mobility, enhanced Lombardi model [17] is used for perpendicular field-dependent mobility, and Caughey–Thomas model [18] is used for lateral field-dependent mobility. Temperature dependence is included in the mobility models and saturation velocity. The reduced thermal conductivity of the fin is considered according to (1).

The corresponding simulated lattice temperature distribution at high drain voltage (0.9 V) and gate bias of 0.9 V for the bulk FinFET is shown in Fig. 4(a). At different gate bias, the maximum lattice temperature and average temperature of the fin resulting from the electrothermal simulations are shown in Fig. 4(b), which show how device temperature is evolving as a function of V_g. The corresponding I_d–V_g characteristics are shown in Fig. 5, where the plotted I_d is the total drain current divided by the effective fin width, i.e., $W = 2H_F + W_F$. The corresponding simulation results for the SOI FinFET are shown in Figs. 6 and 7. Due to the much lower thermal

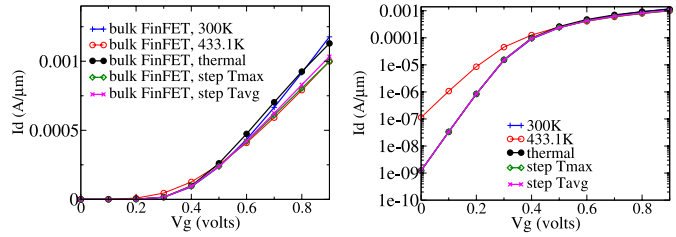

Fig. 5. Simulated I_d–V_g characteristics at high drain voltage for the bulk FinFET. Left: on linear scale. Right: on logarithmic scale. The self-heating produces lower ON-current; however, its impact is different from uniform temperature simulations.

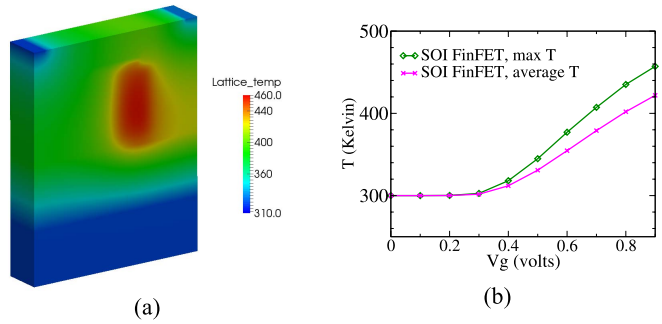

(a) (b)

Fig. 6. Simulation results for the SOI FinFET. (a) Lattice temperature profile in the middle at $V_g = V_d = 0.9$ V. (b) Maximum temperature and average temperature in the fin at high drain voltage.

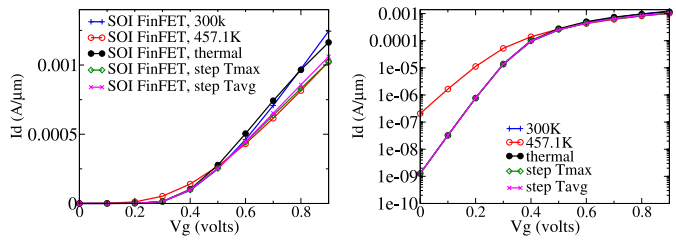

Fig. 7. Simulated I_d–V_g characteristics at high drain voltage for the SOI FinFET. Left: on linear scale; Right: on logarithmic scale. The self-heating produces lower ON-current, however, its impact is different from uniform temperature simulations.

conductivity of the fin, a significant hot spot is produced near the drain, with peak lattice temperature reaching 457 K in the SOI FinFET and reaching 433 K in the bulk FinFET. This also indicates strong temperature gradients in the region, which affect the local current density through the additional part related to thermal gradient ∇T_L

$$J_n = qn\mu_n E_n + k\mu_n T_L \nabla n + k\mu_n n \nabla T_L \tag{2}$$

where n is the electron density, μ_n is the electron mobility, k is the Boltzmann constant.

For comparison, simulations without self-heating, where the lattice temperature is geometrically uniform in the device region, are performed. Results are presented at uniform room temperature and at the temperature corresponding to the maximum temperature observed within the device during the electrothermal simulations. In addition, we run simulations without self-heating at a constant temperature defined by the maximum temperature [as green lines in Figs. 4(b) and 6(b)], and defined by the average temperature in the fin [as purple lines in Figs. 4(b) and 6(b)], at each individual

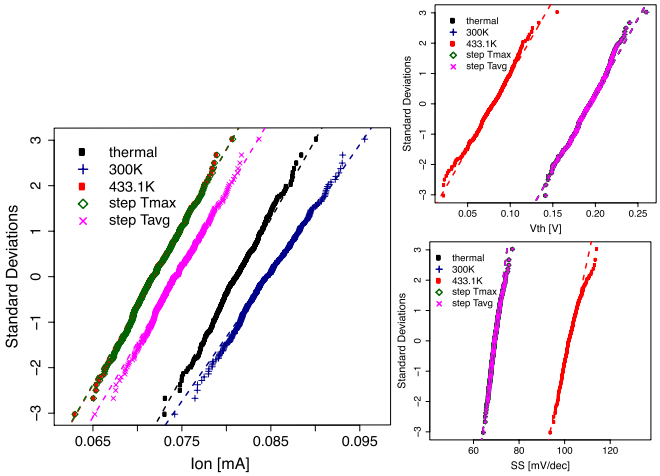

Fig. 8. Comparison of the statistical distribution of ON-current for the bulk FinFET obtained from the electrothermal simulations with uniform temperature simulation results without self-heating. Insets: threshold voltage and subthreshold slope. All at high drain bias. Impact of self-heating on the statistical distribution of the ON-current is clearly shown, especially the reduction of the I_{ON} variability.

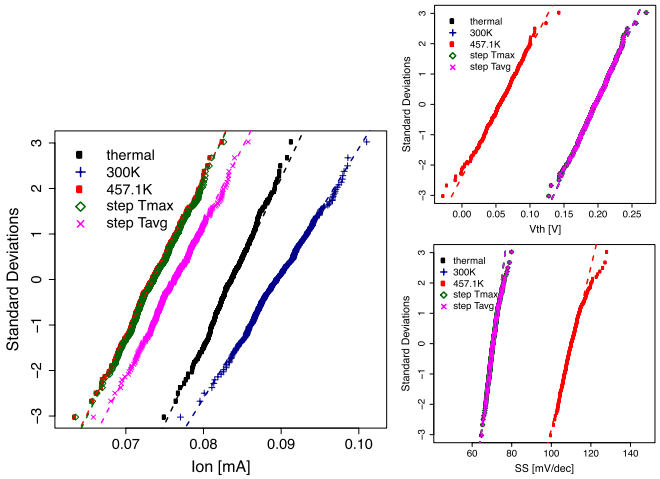

Fig. 9. Comparison of the statistical distribution of ON-current for the SOI FinFET obtained from the electrothermal simulations with uniform temperature simulation results without self-heating. Insets: threshold voltage and subthreshold slope. All at high drain bias. Impact of self-heating on the statistical distribution of the ON-current is clearly shown, especially the reduction of the I_{ON} variability.

V_d and V_g bias condition obtained from the electrothermal simulations, which is denoted as step $T_{\max}$ and step T_{avg}, respectively. As shown in Figs. 5 and 7, the self-heating produces higher drain current in the V_g range of 0.4–0.7 V, the reason being that the impact on the Vth/SS is stronger than the mobility reduction.

B. Statistical Variability Simulations

The electrothermal simulation module is integrated seamlessly with the statistical variability simulation capability of GARAND. LER is modeled with the assumption that it follows a Gaussian autocorrelation function [19]. Both GER and fin edge roughness (FER) are included in the simulations, with three times root-mean-square deviation of the gate edge position of $3\Delta = 2$ nm and a correlation length of $\Lambda = 30$ nm. In the modeling of MGG, we assume a TiN metal gate with an average grain diameter of 5 nm and two major grain orientations which lead to a work-function (WF) difference of 0.2 V, and the probability for the lower and higher WF is 0.4 and 0.6, respectively [20]–[23]. For both bulk and SOI FinFET examples, ensembles of 400 microscopically different devices were simulated using the automated GSS cluster simulation technology, including combined sources of variability GER, FER, and MGG.

The standard deviations of the threshold voltage are very similar for the two FinFETs: 19 and 21 mV for the bulk and the SOI FinFETs, respectively. Correspondingly, the matching factors (defined as $A_{VT} = \sigma_{\Delta V_T}\sqrt{\mathrm{WL}} = \sqrt{2}\sigma_{V_T}\sqrt{\mathrm{WL}}$) for the two FinFETs are 1.14 and 1.25 mV $\cdot$ μm, respectively, where W in this case is the effective fin width, $W = 2H_F + W_F$.

IV. Electrothermal Statistical Variability Study

Electrothermal simulations have been performed on the FinFETs with statistical variations as detailed in Section III-B, and corresponding figures of merit including ON-current (I_{ON}), threshold voltage (V_{th}), the subthreshold slope (SS), and the OFF-current (I_{OFF}) have been extracted. Fig. 8 shows the statistical distribution of the figures of merit at drain bias of 0.9 V for the bulk FinFET obtained from the electrothermal simulations, and the analogous distributions for the SOI FinFET are shown in Fig. 9. For comparison, the results from variability simulations without self-heating for different cases as specified in Section III-A are also plotted in these two figures. In these comparison simulations, the lattice temperature is geometrically uniform in the device region, and the value from the characteristics of the nominal device is used as the nominal temperature. Here, Vth is VTsat and SS is extracted from the saturation curve.

It is not surprising that the self-heating only affects the distribution of the ON-current (I_{ON}) in the case of dc operation. The rest of the figures of merit are related to the subthreshold region where the self-heating effects are minimal, therefore, there is no observable difference between the uniform room temperature simulation and the electrothermal simulations. What is somewhat surprising is that the self-heating significantly reduces the I_{ON} variability according to the electrothermal simulations. The effect is more pronounced in the SOI FinFET where the self-heating is stronger. The explanation of this effect is related to a negative feedback associated with the statistical distribution of I_{ON}. Devices from the higher current part of the statistical distribution suffer more from the self-heating and their current is more reduced compared with the devices from the lower end of the statistical distribution. In order to illustrate this point, Fig. 10 compares the temperature distribution of the two bulk FinFETs from Fig. 8 with the highest and lowest currents in the distribution. The maximum temperature in the first case is 440.8 K and the maximum temperature in the second case is 410.8 K, because microscopically the structures of the two cases are different due to different GER, LER, and MGG patterns, leading to field and current density differences, and the corresponding differences in the heat generation.

The averages and the standard deviations of I_{ON} in the five types of simulations presented in Figs. 8 and 9 are

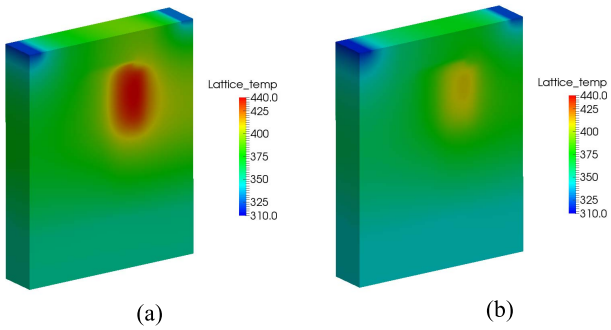

Fig. 10. Temperature distribution of the two bulk FinFETs from Fig. 8(a) with (a) highest and (b) lowest currents in the distribution.

TABLE III
MEAN AND STANDARD DEVIATION OF ON-CURRENT, EXTRACTED FROM SIMULATIONS FOR A STATISTICAL ENSEMBLE OF 400

I_{on} (mA)		*Bulk FinFET*	*SOI FinFET*
Uniform 300K	**μ**	0.0847	0.0896
	σ	0.0034	0.0037
	σ_{normal}	4.0%	4.1%
Electro-thermal simulations	**μ**	0.0813	0.0838
	σ	0.0027	0.0026
	σ_{normal}	3.3%	3.1%
Uniform peak temperature	**μ**	0.0719	0.0736
	σ	0.0028	0.0029
	σ_{normal}	3.9%	3.9%
Step Tmax (maximum temperature at each individual step)	**μ**	0.0719	0.0736
	σ	0.0028	0.0029
	σ_{normal}	3.9%	3.9%
Step Tavg (average temperature in the fin at each individual step)	**μ**	0.0744	0.0764
	σ	0.0029	0.0030
	σ_{normal}	3.9%	3.9%

μ: mean; σ: standard deviation; σ_{normal}: normalized standard deviation.

summarized in Table III. It verifies that both the average (μ) and the standard deviation (σ) for I_{ON} have been reduced because of the self-heating effects. Due to the thermal isolation of the buried oxide, these effects are stronger in the SOI FinFET, where standard deviation of I_{ON} reduced 1.1 μA from 3.7 μA at uniform room temperature, according to the results from electrothermal simulations. For bulk FinFET, the standard deviation of I_{ON} reduced 0.7 μA from 3.4 μA at uniform room temperature according to results from electrothermal simulations. Looking at the normalized standard deviation of I_{ON}, electrothermal simulations give the results of 3% for both bulk and SOI FinFETs. Contrarily, a uniform increase in the temperature has a different impact: the reduction of average I_{ON} is larger, while the standard deviation is comparable, therefore statistical variability is enlarged from

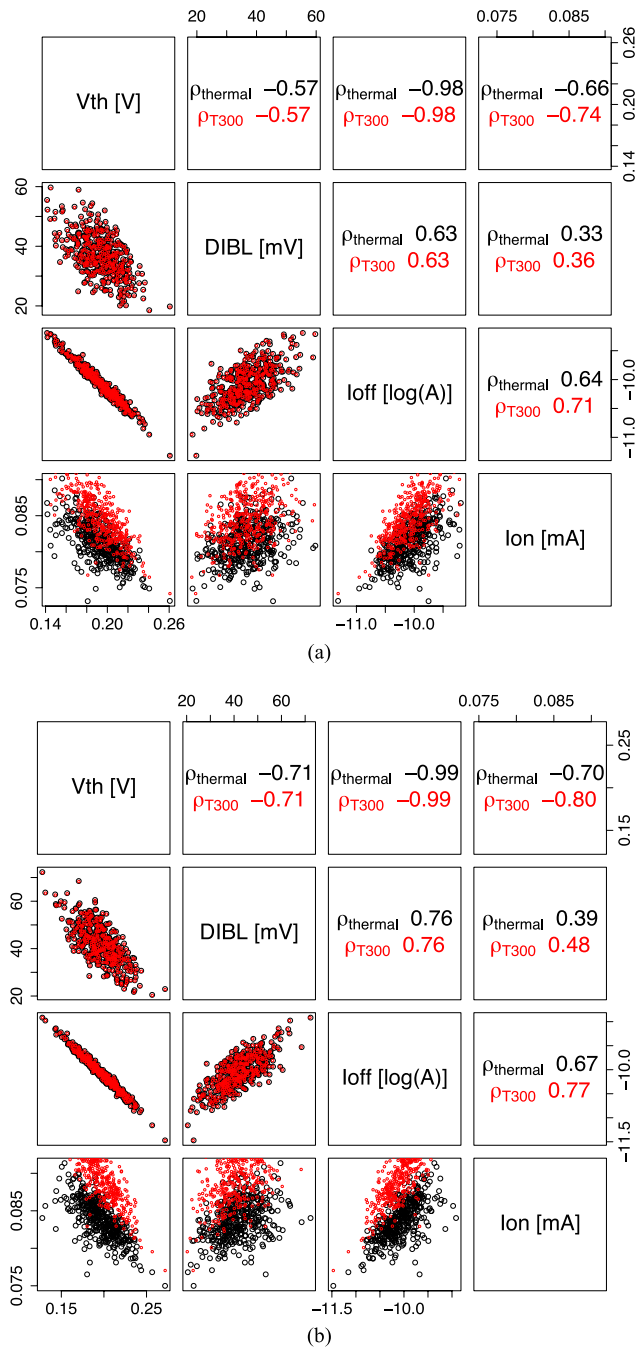

Fig. 11. Correlation between the figures of merit in the electrothermal statistical simulation (in black) of (a) bulk and (b) SOI FinFETs, comparing with results with uniform lattice temperature at 300 K (in red). The correlation coefficients can be read diagonally. The self-heating strongly affects the correlation between I_{ON} and all other figures of merit.

the viewpoint of the normalized standard deviation (~4% both for the bulk and the SOI FinFET examples). This means uniform increase of temperature in the whole device region cannot accurately reflect the trends of I_{ON} variation, and the temperature gradient in the channel needs to be included when considering the full picture of self-heating effects.

As could be expected, the self-heating strongly affects the correlation between I_{ON} and all other figures of merit. This is shown in Fig. 11 for both FinFETs, where the correlation coefficients can be read diagonally. For example, for the bulk FinFET the correlation coefficient between I_{ON} and V_{th}

changes from −0.66 at uniform room temperature to −0.74 according to the electrothermal simulation, while for the SOI FinFET, change of this correlation coefficient due to self-heating is larger (from −0.70 to −0.80). These will provide useful information for compact modeling.

V. Conclusion

In this paper, we present results that obtained from the electrothermal simulation of statistical variability in bulk and SOI FinFETs. The electrothermal simulations consider the impact of the fin geometry on the thermal conductivity. The reduced thermal conductivity has a dramatic effect on the self-heating, raising the peak temperature to 433 K in the case of bulk FinFETs and to 457 K in the case of SOI FinFETs. The self-heating has a strong impact in reducing the ON-current variability but does not significantly affect the threshold voltage, subthreshold slope, and OFF current variability. This in turn affects the correlation between the ON-current distribution and the distributions of the rest of the figures of merit. This paper focuses on the dc operation, while the impact on variability in circuit switching will strongly depend on the workload. A negative feedback between the current variability and the self-heating is indicated from our simulation.

In contrast, uniform increase of temperature in the whole device region cannot accurately reflect the trends of I_{ON} variation, and the temperature gradient in the channel needs to be included when considering the full picture of self-heating effects.

References

[1] C. Auth *et al.*, "A 22 nm high performance and low-power CMOS technology featuring fully-depleted tri-gate transistors, self-aligned contacts and high density MIM capacitors," in *Proc. VLSI Technol. Symp.*, Jun. 2012, pp. 131–132.

[2] S. Kumar *et al.*, "Self-consistent and efficient electro-thermal analysis for poly/metal gate FinFETs," in *Proc. IEDM*, Dec. 2006, pp. 1–4.

[3] S. Kolluri, K. Endo, E. Suzuki, and K. Banerjee, "Modeling and analysis of self-heating in FinFET devices for improved circuit and EOS/ESD performance," in *Proc. IEEE IEDM*, Dec. 2007, pp. 177–180.

[4] C. Xu, S. K. Kolluri, K. Endo, and K. Banerjee, "Analytical thermal model for self-heating in advanced FinFET devices with implications for design and reliability," *IEEE Trans. Comput.-Aided Design Integr. Circuits Syst.*, vol. 32, no. 7, pp. 1045–1058, Jul. 2013.

[5] M. Shrivastava *et al.*, "Physical insight toward heat transport and an improved electrothermal modeling framework for FinFET architectures," *IEEE Trans. Electron Devices*, vol. 59, no. 5, pp. 1353–1363, May 2012.

[6] M. Braccioli, G. Curatola, Y. Yang, E. Sangiorgi, and C. Fiegna, "Simulation of self-heating effects in 30 nm gate length FinFET," in *Proc. 9th Int. Conf. ULIS*, Mar. 2008, pp. 71–74.

[7] A. J. Scholten *et al.*, "Experimental assessment of self-heating in SOI FinFETs," in *Proc. IEEE IEDM*, Dec. 2009, pp. 1–4.

[8] L. Wang *et al.*, "3D coupled electro-thermal simulations for SOI FinFET with statistical variations including the fin shape dependence of the thermal conductivity," in *Proc. 12th IEEE Int. Conf. Solid-State Integr. Circuit Technol. (ICSICT)*, Oct. 2014, pp. 1–3.

[9] J. Mazurier *et al.*, "Drain current variability and MOSFET parameters correlations in planar FDSOI technology," in *Proc. IEEE IEDM*, Dec. 2011, pp. 25.5.1–25.5.4.

[10] J. Mazurier *et al.*, "On the variability in planar FDSOI technology: From MOSFETs to SRAM cells," *IEEE Trans. Electron Devices*, vol. 58, no. 8, pp. 2326–2336, Aug. 2011.

[11] A. R. Brown, N. Daval, K. K. Bourdelle, B.-Y. Nguyen, and A. Asenov, "Comparative simulation analysis of process-induced variability in nanoscale SOI and bulk trigate FinFETs," *IEEE Trans. Electron Devices*, vol. 60, no. 11, pp. 3611–3617, Nov. 2013.

[12] (2014). *GARAND Statistical 3D TCAD Simulator*. [Online]. Available: http://www.GoldStandardSimulations.com/products/garand/

[13] X. Wang, B. Cheng, A. R. Brown, C. Millar, and A. Asenov, "Statistical variability in 14-nm node SOI FinFETs and its impact on corresponding 6T-SRAM cell design," in *Proc. ESSDERC*, Sep. 2012, pp. 113–116.

[14] B. Cheng, A. R. Brown, X. Wang, and A. Asenov, "Statistical variability study of a 10 nm gate length SOI FinFET device," in *Proc. IEEE Silicon Nanoelectron. Workshop*, Jun. 2012, pp. 1–2.

[15] D. Vasileska, K. Raleva, and S. M. Goodnick, "Electrothermal studies of FD SOI devices that utilize a new theoretical model for the temperature and thickness dependence of the thermal conductivity," *IEEE Trans. Electron Devices*, vol. 57, no. 3, pp. 726–728, Mar. 2010.

[16] G. Masetti, M. Severi, and S. Solmi, "Modeling of carrier mobility against carrier concentration in arsenic-, phosphorus-, and boron-doped silicon," *IEEE Trans. Electron Devices*, vol. 30, no. 7, pp. 764–769, Jul. 1983.

[17] C. Lombardi, S. Manzini, A. Saporito, and M. Vanzi, "A physically based mobility model for numerical simulation of nonplanar devices," *IEEE Trans. Comput.-Aided Design Integr. Circuits Syst.*, vol. 7, no. 11, pp. 1164–1171, Nov. 1988.

[18] D. M. Caughey and R. E. Thomas, "Carrier mobilities in silicon empirically related to doping and field," *Proc. IEEE*, vol. 55, no. 12, pp. 2192–2193, Dec. 1967.

[19] A. Asenov, S. Kaya, and A. R. Brown, "Intrinsic parameter fluctuations in decananometer MOSFETs introduced by gate line edge roughness," *IEEE Trans. Electron Devices*, vol. 50, no. 5, pp. 1254–1260, May 2003.

[20] H. Dadgour, K. Endo, V. De, and K. Banerjee, "Modeling and analysis of grain-orientation effects in emerging metal-gate devices and implications for SRAM reliability," in *Proc. IEEE IEDM*, Dec. 2008, pp. 1–4.

[21] K. Ohmori *et al.*, "Impact of additional factors in threshold voltage variability of metal/high-*k* gate stacks and its reduction by controlling crystalline structure and grain size in the metal gates," in *Proc. IEEE IEDM*, Dec. 2008, pp. 1–4.

[22] A. R. Brown, N. M. Idris, J. R. Watling, and A. Asenov, "Impact of metal gate granularity on threshold voltage variability: A full-scale three-dimensional statistical simulation study," *IEEE Electron Device Lett.*, vol. 31, no. 11, pp. 1199–1201, Nov. 2010.

[23] X. Wang, A. R. Brown, N. Idris, S. Markov, G. Roy, and A. Asenov, "Statistical threshold-voltage variability in scaled decananometer bulk HKMG MOSFETs: A full-scale 3-D simulation scaling study," *IEEE Trans. Electron Devices*, vol. 58, no. 8, pp. 2293–2301, Aug. 2011.

Liping Wang received the B.S. and Ph.D. degrees in electronics from Xi'an Jiaotong University, Xi'an, China, in 1995 and 2000, respectively.

She held a post-doctoral position with the Cavendish Laboratory, Cambridge University, Cambridge, U.K., from 2000 to 2002. She joined the School of Engineering, University of Glasgow, Glasgow, U.K., in 2011, after more than seven years of industrial experience with a specialized CAD software company in London.

Andrew R. Brown (M'09) received the B.Eng. (Hons.) degree in electronics and electrical engineering from the University of Glasgow, Glasgow, U.K., in 1992.

He is currently the Chief Developer of the TCAD Device Simulator Garand with Gold Standard Simulations, Ltd., Glasgow.

Mihail Nedjalkov received the master's degree in physics from Sofia University, Bulgaria, and the Ph.D., Habilitation, and D.Sc. degrees from the Bulgarian Academy of Sciences (BAS), Sofia, Bulgaria, in 1990, 2001, and 2011, respectively.

He is currently an Associate Professor with the Institute of Information and Communication Technologies, BAS, and a Visiting Scientist with the Institute for Microelectronics, Technische Universität Wien, Vienna, Austria.

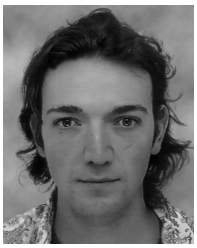

Craig Alexander received the M.Sc. degree in joint physics and astronomy from the University of Glasgow, Glasgow, U.K., in 2001, and the Ph.D. degree from the Device Modeling Group, University of Glasgow.

He joined Gold Standard Simulations, Ltd., Glasgow, in 2012, where he leads the Monte–Carlo simulation development.

Binjie Cheng (M'11) received the B.S. and M.S. degrees in optical and physical electronic engineering and the Ph.D. degree in electronic science and technology from Xi'an Jiaotong University, Xi'an, China, in 1994, 1997, and 2000, respectively.

He was a Research Fellow with the School of Engineering, University of Glasgow, Glasgow, U.K. He is currently with Gold Standard Simulations, Ltd., Glasgow.

Campbell Millar (M'09) received the B.Eng. degree in electronics engineering and music and the Ph.D. degree from the University of Glasgow, Glasgow, U.K., in 1999 and 2003, respectively.

He was a Senior Research Fellow with the School of Engineering, University of Glasgow. He joined Gold Standard Simulations Ltd., Glasgow, where he is currently the Vice President of Software Development.

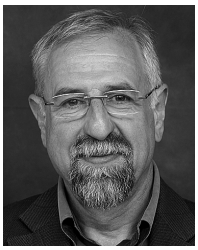

Asen Asenov (M'96–SM'05–F'11) received the Ph.D. degree in solid-state physics from the Bulgarian Academy of Sciences, Sofia, Bulgaria, in 1989.

He is currently the CEO with Gold Standard Simulations Ltd., Glasgow, U.K., and a James Watt Professor of Electrical Engineering with Glasgow University, Glasgow.